OXFORD GENETICS

GENETICS, 2022, 221(1), iyac043
https://doi.org/10.1093/genetics/iyac043
Advance Access Publication Date: 17 March 2022
Investigation

STRIPAK regulation of katanin microtubule severing in the *Caenorhabditis elegans* embryo

Tammy Lu, Ryan B. Smit, Hanifa Soueid, Paul E. Mains *

Department of Biochemistry and Molecular Biology, Alberta Children's Hospital Research Institute, University of Calgary, Calgary, AL T2N 4N1, Canada

*Corresponding author: Department of Biochemistry and Molecular Biology, University of Calgary, 3330 Hospital Dr. NW, Calgary, AL T2N 4N1, Canada. Email: mains@ucalgary.ca

Abstract

Microtubule severing plays important role in cell structure and cell division. The microtubule severing protein katanin, composed of the MEI-1/MEI-2 subunits in *Caenorhabditis elegans*, is required for oocyte meiotic spindle formation; however, it must be inactivated for mitosis to proceed as continued katanin expression is lethal. Katanin activity is regulated by 2 ubiquitin-based protein degradation pathways. Another ubiquitin ligase, HECD-1, the homolog of human HECTD1/HECT domain E3 ubiquitin protein ligase 1, regulates katanin activity without affecting katanin levels. In other organisms, HECD-1 is a component of the striatin-interacting kinase phosphatase complex, which affects cell proliferation and a variety of signaling pathways. Here we conducted a systematic screen of how mutations in striatin-interacting kinase phosphatase components affect katanin function in *C. elegans*. Striatin-interacting kinase phosphatase core components (FARL-11, CASH-1, LET-92, and GCK-1) were katanin inhibitors in mitosis and activators in meiosis, much like HECD-1. By contrast, variable components (SLMP-1, OTUB-2) functioned as activators of katanin activity in mitosis, indicating they may function to alter striatin-interacting kinase phosphatase core function. The core component CCM-3 acted as an inhibitor at both divisions, while other components (MOB-4, C49H3.6) showed weak interactions with katanin mutants. Additional experiments indicate that katanin may be involved with the centralspindlin complex and a tubulin chaperone. HECD-1 shows ubiquitous expression in the cytoplasm throughout meiosis and early development. The differing functions of the different subunits could contribute to the diverse functions of the striatin-interacting kinase phosphatase complex in *C. elegans* and other organisms.

Keywords: *C. elegans*; embryo; STRIPAK; katanin; microtubules; meiosis; mitosis; HECTD1 ubiquitin ligase

Introduction

The meiotic and the mitotic spindles of the *Caenorhabditis elegans* embryo, like those of other organisms, differ in many respects (Muller-Reichert *et al.* 2010; Mullen *et al.* 2019). For example, meiotic spindles are composed of short microtubules nucleated near the chromatin and are found adjacent to the cortex for polar body extrusion. Mitotic spindles are much larger and central, with long microtubules nucleated by centrosomes contributed by the sperm. Because of the differences, each division requires factors specific to that type of spindle. Furthermore, these factors require precise temporal regulation as the time from the end of meiosis to formation to the first mitotic cleavage is only 15 min in *C. elegans* (McCarter *et al.* 1999). An example of a *C. elegans* meiotic-specific factor is the katanin microtubule-severing complex, encoded by the *mei-1* and *mei-2* genes (Mains *et al.* 1990a; Clark-Maguire and Mains 1994; Srayko *et al.* 2000). While essential for meiosis, postmeiotic katanin activity is lethal. Multiple layers of regulation restrict katanin activity to meiosis, which include protein ubiquitination and regulation of enzymatic activity by phosphorylation (Furukawa *et al.* 2003; Pintard *et al.* 2003; Xu *et al.* 2003; Stitzel *et al.* 2007; Joly *et al.* 2020).

The katanin microtubule-severing complex remodels oocyte meiotic spindle microtubules into short and dense arrays (McNally *et al.* 2006; McNally and Roll-Mecak 2018; Joly *et al.* 2020). Katanin and related microtubule-severing complexes are involved in a variety of biological processes including axon and cilia development, cell division and cell migration, and are implicated in diseases like microcephaly and cancer (Karabay *et al.* 2004; Lu *et al.* 2004; Zhang *et al.* 2007; Hu *et al.* 2014; Baas *et al.* 2016; Fu *et al.* 2018; McNally and Roll-Mecak 2018;). Katanin is a hexamer made of 2 components, a catalytic subunit (p60) and a regulatory subunit (p80). Katanin p60 hydrolyzes ATP and severs microtubules, while p80 is necessary for microtubule binding, bundling and stabilizing p60 (McNally and Vale 1993; Connolly *et al.* 2014; McNally *et al.* 2014; Joly *et al.* 2016; McNally and Roll-Mecak 2018). The 2 new fragments of a severed microtubule each serve as stable bases for microtubule growth, increasing the total microtubule mass during acentrosomal spindle formation in *C. elegans* meiosis (McNally *et al.* 2006; Srayko *et al.* 2006; Joly *et al.* 2016). Katanin microtubule severing also arranges microtubules in parallel by cutting at areas of microtubule intersection (McNally *et al.* 2014; McNally and Roll-Mecak 2018). MEI-1 and MEI-2 colocalize at the spindle poles and on the chromosomes

Received: February 04, 2022. **Accepted:** March 15, 2022

during meiosis and each subunit is required for the other's localization (Clark-Maguire and Mains 1994; Srayko *et al.* 2000).

Lack of katanin microtubule severing in *C. elegans* meiosis is lethal, and results in long but sparse microtubules, apolar spindles and defects in polar body formation (Mains *et al.* 1990a; Srayko *et al.* 2006; Connolly *et al.* 2014; Joly *et al.* 2016; Schlientz and Bowerman 2020). By mitosis, paternally contributed centrosomes nucleate longer microtubules. MEI-1 and MEI-2 levels quickly decrease prior to the first cleavage (Clark-Maguire and Mains 1994; Srayko *et al.* 2000; Lu and Mains 2007). Indeed, mutations resulting in continued expression of katanin into mitosis are lethal, resulting in short and misoriented spindles and improper cytokinesis. Ectopic MEI-1 and MEI-2 during mitosis are found at the centrosomes and chromosomes (Clark-Maguire and Mains 1994; Srayko *et al.* 2000). The only other embryonic function attributed to katanin occurs much later in embryo development, where it has subtle effects on muscle organization (Wilson *et al.* 2012). Zygotic loss has no effects on viability (Mains *et al.* 1990a).

Caenorhabditis elegans have adopted multiple forms of katanin regulation during the meiotic to mitotic transition; the best understood are the multisubunit cullin-based E3 ubiquitin ligases (Furukawa *et al.* 2003; Pintard *et al.* 2003; Xu *et al.* 2003). These tag proteins with ubiquitin to mark them for proteosomal degradation (Metzger *et al.* 2012; Akutsu *et al.* 2016; Morreale and Walden 2016). The cullin subunit acts as a scaffold to recruit other components, including substrate recognition subunits. Katanin is regulated by 2 cullin-based E3 ubiquitin ligases that act in parallel (Fig. 1a) (Lu and Mains 2007; Beard *et al.* 2016). Following meiosis, katanin is primarily degraded by a CUL-3 based E3 ubiquitin ligase using the MEL-26 substrate recognition subunit that binds MEI-1/katanin. (Furukawa *et al.* 2003; Pintard *et al.* 2003; Xu *et al.* 2003). A second pathway contributes relatively less to MEI-1 degradation and results in MEI-1 phosphorylation by MBK-2/Mini Brain Kinase (Stitzel *et al.* 2007; Joly *et al.* 2020) and degradation by E3 ubiquitin ligase based on CUL-2 and an unknown substrate adaptor (Lu and Mains 2007; Beard *et al.* 2016). Maximal ectopic MEI-1 levels during mitotic cleavages requires mutations in both the *cul-3/mel-26* and the *cul-2/mbk-2* pathways (Lu and Mains 2007; Beard *et al.* 2016).

Other katanin regulators affect katanin activity without impacting MEI-1 levels. MBK-2 phosphorylation also inhibits katanin enzymatic activity independent of its role in MEI-1 degradation (Loughlin *et al.* 2011; Joly *et al.* 2020). PPFR-1/Protein Phosphatase Four Regulator Subunit acts to dephosphorylate MEI-1 to increase its meiotic activity, and like MEI-1, PPFR-1 is targeted by MEL-26 for postmeiotic degradation (Han *et al.* 2009; Gomes *et al.* 2013). By contrast, a third E3 ligase, HECD-1, is a HECT (Homologous to the E6AP Carboxyl Terminus) that regulates katanin function without affecting MEI-1 levels (Beard *et al.* 2016). HECD-1 switches from activating microtubule severing at meiosis to inhibiting microtubule severing in mitosis, perhaps by biasing katanin to prefer meiotic over mitotic spindles.

HECT E3 ligases use lysine 63 (K63) ubiquitin linkages rather than K48 as do cullin-based ligases (Metzger *et al.* 2012; Morreale and Walden 2016; Wang *et al.* 2020). These K63 linkages usually result in the change of protein localization rather than degradation (Akutsu *et al.* 2016). For example, Tran *et al.* (2013) found that elimination of mammalian HECTD1 changed the localization of a ß-catenin degradation complex from the cytoplasm to the cortex in cultured cells. Sarkar and Zohn (2012) found that loss of HECTD1 resulted in heat shock protein 90 moving from the nucleus and cytoplasm to the plasma membrane in mutant mouse placenta. However, Beard *et al.* (2016) saw no detectable changes in either the location (or levels) of MEI-1, MEI-2, MEL-26, or PPFR-1 in *hecd-1* backgrounds. This suggests that HECD-1 is interacting with unknown katanin regulators in *C. elegans*.

HECT ubiquitin ligases can function in physical association with the striatin-interacting kinase phosphatase (STRIPAK) complex, whose components represent candidates that could mediate interactions between HECD-1 and katanin. The STRIPAK complex is conserved from fungi to mammals. STRIPAK acts in diverse processes including WNT, Hippo and JNK signaling, cell migration, apoptosis, endocytosis, cell septation, membranous tubule formation and vascular development and may serve to coordinate actions of different signaling pathways (Hwang and Pallas 2014; Shi *et al.* 2016; Kuck *et al.* 2019; Kuck and Stein 2021). In the context of WNT signaling, Tran *et al.* (2013) identified HECTD1 and STRIPAK through coimmunoprecipitation of Trabid/OTUD7, a K63 deubiquitinase that counteracts the HECTD1 K63 ubiquitinylation (Kean *et al.* 2011; Tran *et al.* 2013). The STRIPAK complex includes Striatin as the main scaffolding component (Fig. 1b). A protein phosphatase (PP2A) binds to the N-terminal region of striatin. On the striatin C-terminal region, cerebral cavernous malformations 3 (CCM3) bridges the germinal center kinase III (GCKIII). These subunits, together with the MOB kinase activator-like 3 (Mob3) and STRIP1/2, make up the core components of STRIPAK. STRIP1/2 is responsible for attaching variable STRIPAK components. Variable components include HECTD1, sarcolemma-associated protein (SLMAP), N-terminal like cortactin-binding protein 2 (CTTNBP2NL) and the Trabid/OTUD7 deubiquitinase (Goudreault *et al.* 2009; Hwang and Pallas 2014; Shi *et al.* 2016). STRIPAK components are also found in STRIPAK-like complexes and as subcomplexes before assembling (Tran *et al.* 2013; Elramli *et al.* 2019; Kuck *et al.* 2019).

STRIPAK functions in a range of developmental processes in *C. elegans* including excretory canal extension, cytokinesis, vesicle trafficking, and endocytosis (Lant *et al.* 2015; Pal *et al.* 2017). Coimmunoprecipitation of GCK-1 (GCKIII) by Pal *et al.* (2017) identified the *C. elegans* STRIPAK complex (Fig. 1b). These include FARL-11 (Strip1/2), SLMP-1 (SLMAP, previously designated M4.1 in *C. elegans*), LET-92 (PP2A catalytic subunit α), PAA-1 (PP2A scaffold subunit α), CASH-1 (Striatin) and CCM-3. Common phenotypes include low brood size due to a collapsed rachis (the shared cytoplasm of dividing germline stem cells) and multinucleated oocytes (Pal *et al.* 2017). Variable components of the STRIPAK complex such as C49H3.9 (CTTNBP2NL), HECD-1 and OTUB-2 (Trabid deubiquitinase) were not present in the *C. elegans* GCK-1 coimmunoprecipitation experiments of Pal *et al.* (2017). These were found in mammalian STRIPAK based on Trabid/OTUD7 immunoprecipitates of Tran *et al.* (2013), who correspondingly did not isolate GCK-1/GCKIII. This may indicate the variable composition of STRIPAK complexes or the transient nature of their associations.

STRIPAK complexes can be associated with microtubules, where they could potentially interact with katanin. Sakuma *et al.* (2015) showed that *Drosophila* STRIP2 (*C. elegans* FARL-11) and the tubulin folding cofactor D/TBCD (TBCD-1) physically interacted with one another and mutations had similar phenotypes. The tubulin-folding cofactor D mediates the biogenesis and degradation of α/ß heterodimers (Nithianantham *et al.* 2015). Other STRIPAK components associated with microtubules, spindles or centrosomes, include *Drosophila* FAM40a and FAM40b (FARL-11) (Bai *et al.* 2011), mammalian MOBKL3 (MOB-4) and SLMAP (SLMP-1) (Frost *et al.* 2012; Hwang and Pallas 2014). *Caenorhabditis elegans* LET-92 (PP2A) localizes toward the meiotic spindle poles and chromosomes (Bel Borja *et al.* 2020).

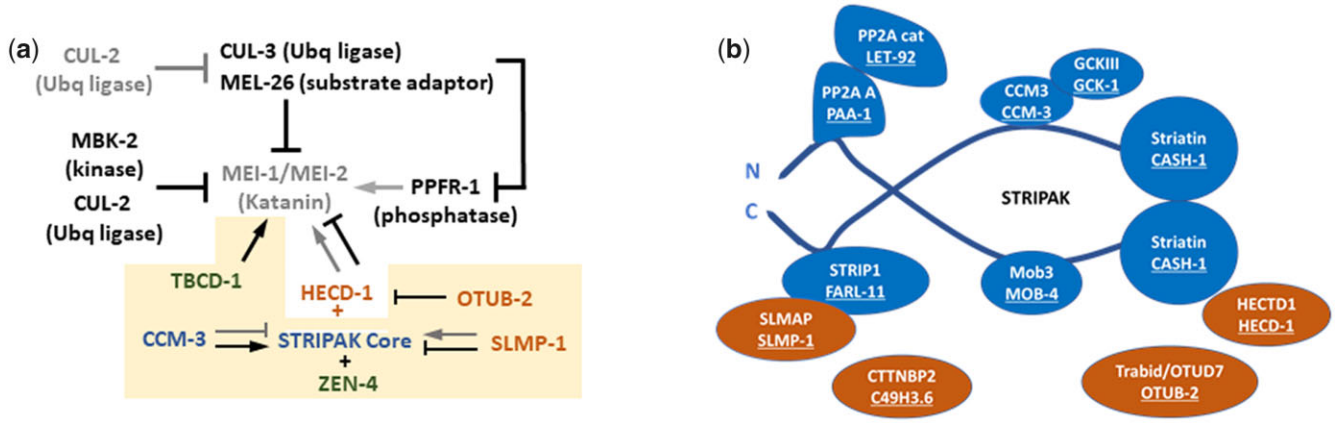

(c)

Summary of New Results

STRIPAK Core / STRIPAK Variable Components / STRIPAK Interactors

Meiosis (katanin normally active)		Mitosis (katanin normally inactive)	
Katanin activator *mei-2* enhancement	*farl-11, cash-1, gck-1, let-92 hecd-1, slmp-1 zen-4, tbcd-1*	**Katanin activator** *mel-26* rescue	*slmp-1, otub-2 tbcd-1*
Katanin inhibitor *mei-2* rescue	*ccm-3*	**Katanin inhibitor** *mel-26* enhancement	*hecd-1 ccm-3, farl-11, cash-1, gck-1, let-92 zen-4, kri-1*
Weak or no interaction	*otub-2*	**Weak or no interaction**	*mob-4 C49H3.6*

Fig. 1. STRIPAK components and katanin regulation. a) Summary of the genetic pathway of MEI-1/MEI-2 regulation. In the core MEI-1 regulatory pathway (in the upper part of the figure) gray lettering indicates proteins active in meiosis while black indicates mitotic activity. Positive (arrows) and negative (T-bars) genetic interactions use the same color coding. Genetic interactions in the yellow shaded section are the new results described in this manuscript. STRIPAK core components are in blue and variable components are in orange. Note that interactions with katanin described in the text are the net sum of a gene's activity and that of its downstream targets. For example, SMLP-1 is a net activator of mitotic katanin as it is the inhibitor of an inhibitor as indicated by the 2 black T-bars between SLMP-1 and katanin. b) Diagram indicating physical interactions of the STRIPAK complex with core components in blue and variable in orange. Mammalian component names are shown with their *C. elegans* counterparts below and underlined. The blue line represents Striatin/CASH-1, which acts as the scaffold. c) Summary of the new genetic interactions described in the text (previously known *hecd-1* interactions are included for comparison). Font colors correspond to those in (a) and (b). Note that "inhibitor" or "activator" depends on the sum of all genetics interactions between the gene of interest and *mei-2*.

To determine if STRIPAK is involved with HECD-1 and katanin function in the early *C. elegans* embryo, we made double mutants (or RNAi knockdowns) between mutations that either increase or decrease katanin activity and genes encoding STRIPAK components. Like HECD-1, we found that core components of the STRIPAK complex inhibited katanin in mitosis but acted as activators in meiosis, although CCM-3 functioned as an inhibitor at both divisions. Variable components (SLMP-1, OTUB-2) showed the opposite pattern in mitosis, indicating they may alter STRIPAK function. A tagged HECD-1 allele showed ubiquitous embryonic expression.

Materials and methods

Strains and alleles

Caenorhabditis elegans strains were maintained under standard conditions as specified by Brenner (1974). Worms were grown at 15° on Nematode Growth Media (NGM), spread with OP50 *Escherichia coli* bacteria. Gene descriptions can be found at WormBase. STRIPAK alleles were a gift from the Derry Lab (Lant *et al.* 2015; Pal *et al.* 2017), the Million Mutant Project (Thompson *et al.* 2013) or were obtained from the Caenorhabditis Genetics Center. A detailed list of strains and alleles is included in Supplementary Table 1, which also indicates the number of outcrosses for the Million Mutant Project mutations (Thompson *et al.* 2013). Strains that included mutations with no phenotype on their own were confirmed by PCR using oligonucleotides listed in Supplementary Table 2. Homology of mammalian STRIPAK and other genes tested for katanin interactions, and the nature of the *C. elegans* mutations used in this study, are found in Supplementary Table 3.

Viability of progeny from individual hermaphrodites starting from L4-staged worms were determined as described previously (Mains *et al.* 1990a). Worms were moved to a new NGM plate every 2 days at 15° or 18°, and then the number of eggs vs. hatched larvae were scored 2 days later. Worms at 20°, 23°, 24°, or 25° were moved every day and then scored the day after. Hermaphrodites were transferred until they ceased laying eggs and the hatching rates are the sum of progeny from all broods. For each experiment, >4 hermaphrodites and >400 F1 were

scored. The expected hatching rate of double mutants was calculated by multiplying the hatching rates of the controls. Statistical significance of interactions was calculated using the binomial test on Prism 8. Significance lower than 0.0001 is shown as < 0.0001.

To score males, worms laid eggs for 1 day, and then the parents were removed and F1 worms were scored at the L4 or young adult stage, 2–3 days later. The expected % of males was calculated by multiplying the % hermaphrodites of the single mutant controls and subtracting from 100%. Significance of the interaction was calculated using the 2-tailed binomial test on Prism 8.

RNAi

RNAi protocol was adapted from Kamath and Ahringer (2003) using NGM plates containing 1.5 mM isopropyl β-d-1-thiogalactopyranoside (IPTG) and 50 μg/ml of ampicillin. DHT115(DE3) *E. coli* transformed with an L4440 feeding vector containing the gene of interest was spread on the RNAi plates, allowed to grow overnight and then stored at 4° in the dark. RNAi sequences used are as specified in Supplementary Table 4. Clone identity was confirmed by sequencing.

Depending on the experiment, a minimum of 4 L1 to young adults were placed on RNAi plates and then transferred to new RNAi plates every 12–48 h until no more eggs were laid. Details for each experiment are described in Figure legends. Each experiment was conducted in parallel with controls of the wild type on RNAi and mutant strains grown on bacteria with an empty vector (L4440). The brood number corresponds to the number of plate transfers rather than chronological time. Unlike experiments with mutant strains where hatching rates are the sum of all broods, RNAi hatching rates are reported separately for each brood. We focused on the RNAi broods where the hatching rates of the control and experimental were intermediate (i.e. hypomorphic), with a minimum of 50 progeny. These were generally broods 2 or 3, after RNAi has become effective but before there was complete lethality. The 2-tailed binomial-test on Prism 8 compared observed to expected probability.

HECD-1 CRISPR FLAG tag

To create the *hecd-1(sb142)* FLAG-tagged allele, a 69 bp sequence encoding the *3xflag* epitope was inserted immediately before the *hecd-1* start codon in pBluescript II KS+. The repair template included a silent c.18G>T mutation within the PAM site to prevent subsequent gRNA directed Cas9 cutting of the insertion allele. *hecd-1* homology was 923 bp 5′ of the *3xflag* and 786 bp 3′. This homology extended between a *Hind*III site upstream of the *hecd-1* ATG to the next *BamH*I site within the coding sequence. Gravid wild-type hermaphrodites were injected with 50 ng/μl *eft-3::Cas9*, 12.5 ng/μl pJA58[*dpy-10(cn64)* gRNA], 500 nM *dpy-10(cn64)* oligonucleotide (ARRIBERE *et al.* 2014), 25 ng/μl *hecd-1* gRNA and 50 ng/μl *3xflag::hecd-1(c.18G>T)* repair template plasmid. Oligonucleotides are listed in Supplementary Table 2. Dpy and Rol F1 co-CRISPR progeny were screened by PCR. To ensure only 1 allele was retained in case of biallelic CRISPR, animals with the *3xflag* insertion were crossed to *DnT1(IV; V)*, which balances the *hecd-1* region, and then the *flag::hecd-1* was homozygosed. This yielded the *sb142* allele used in this study, which was confirmed by sequencing.

Antibody staining and imaging

Young adult gravid hermaphrodites were placed on a poly-lysine coated slide in 7.5 μl of water. Control and experimental worms were placed about 2 cm apart on the same slide. 10 × 15 cm coverslips were placed over each group of worms, and then embryos were expelled by gentle tapping with a toothpick. The slide was transferred to dry ice for >60 min and then immersed in liquid nitrogen. After 5 min, the coverslip were flicked off with a razor blade, transferred immediately into −20° methanol for 10 min followed sequentially by acetone, 90% ethanol and 60% ethanol for 3 min each at −20°. This was followed by 30% ethanol and then phosphate buffered saline (Motohashi *et al.* 2006) with 0.5% Triton X-100 (PBX) for 3 min each at room temperature. Slides were blocked with 25% normal goat serum (Jackson ImmunoResearch Lab) plus 25% normal donkey serum (Jackson ImmunoResearch Lab) in PBX for 1 h at 37°. Primary antibodies were diluted in 5% normal donkey serum, 5% normal goat serum and PBX at 1:100 mouse for anti-FLAG (Sigma) and 1:100 for rabbit anti-α-tubulin (Proteintech). Primary antibodies were incubated at 37°. Slides were then washed 4 times in PBX for 10 min each. Secondary 1:200 Texas Red goat anti-mouse (Jackson ImmunoResearch Lab) and 1:100 Alexa488 goat anti-rabbit (Invitrogen) was then incubated at 37° for 45 min and washed 4 times in PBX for 10 minutes each. 3.5 μl of SlowFade Gold Antifade (Invitrogen), which includes DAPI (4′,6-diamidino-2-phenylindole, Invitrogen), to label DNA was used for mounting and coverslips were sealed with clear nail polish.

Images were taken using the Zeiss Axioplan microscope with a 63x (N.A. = 1.4) objective to assess colocalization or a 20x (N.A. = 0.5) objective for quantification of fluorescence levels. Images were photographed with a Hamatsu Orca ER digital camera using Axiovision (4.8.2 software). Exposure settings were kept the same between experiments. Using Image J (Schneider *et al.* 2012), embryos were traced and fluorescence from anti-FLAG staining was measured. The amount of fluorescence of each embryo was normalized to the wild-type control processed on the same slide. Prism 8 was used to calculate one-way analysis of variance (ANOVA) to compare fluorescence between different stages.

Results

To determine if *hecd-1* genetic interactions with katanin could involve the STRIPAK complex, we used either mutants or RNAi by feeding of STRIPAK subunits in the temperature-sensitive (*ts*) *mei-2* or *mel-26* backgrounds. The *ts* mutations allowed us to vary katanin activity with temperature to find the optimal condition for detecting interactions, primarily measured by hatching rates. STRIPAK alleles we used are predicted nulls (Supplementary Table 2, which also includes similarity scores to mammalian proteins). Some STRIPAK mutations are lethal or sterile. As RNAi phenotypes gradually increase over the course of several days, we examined intermediate broods, after RNAi starts to take effect but before the onset of complete lethality or sterility. Note that the "broods" we describe below do not correspond to absolute time, but rather the number of transfers to fresh plates, whose frequency varied with experiment (see Figure Legends). Generally, ranges of 10–80% hatching for the *ts* mutants or RNAi controls were optimal to detect either enhancement or suppression.

To explore STRIPAK interactions with katanin when it is not properly degraded and persists into mitosis, we used *mel-*

26(ct61sb4) (unless otherwise specified, this *mel-26* mutation is used). This is a null allele with an inherently *ts* phenotype of the substrate adapter subunit of CUL-3 ubiquitin ligase (Dow and Mains 1998; Lu and Mains 2007). This allele shows ~15% hatching at 15° but ~2% at 20°. Loss of mitotic inhibitors of katanin function such as *hecd-1* (which by itself has little effect on viability) further increases ectopic katanin function, and so decreases the hatching rate of *mel-26(ct61sb4)* to 0% at 15° (Beard *et al.* 2016). *mel-26* has other (nonlethal) functions in the *C. elegans* embryo that could potentially affect our conclusions (Luke-Glaser *et al.* 2005; Wilson *et al.* 2012). However, the major (perhaps only) essential target of *mel-26* in the embryo is katanin. This is indicated by the strong suppression of *mel-26* by partial depletion of *mei-1* or *mei-2* (Mains *et al.* 1990a; Dow and Mains 1998). Mutations in α and β tubulins that are partially resistant to katanin cleavage efficiently suppress *mel-26*, again indicating that regulation of katanin microtubule severing is the primary function of *mel-26* (Lu *et al.* 2004; Lu and Mains 2005). The temperature-sensitive period for *mel-26* is centered on first embryonic cleavage, indicating that the lethal events are restricted to this narrow window (Mains *et al.* 1990b). Thus the enhancement of lethality we observe likely stems from ectopic microtubule severing rather than other *mel-26* functions. For selected genotypes we demonstrate that the enhancement of *mel-26* lethality by depletion of STRIPAK subunits is suppressed by a *tbb-2* allele, confirming that excess katanin microtubule-severing is the cause of the lethality. We previously demonstrated that the enhancement of *mel-26* by *hecd-1* was similarly suppressed by *tbb-2* (Beard *et al.* 2016). We assume that *tbb-2* blocking *mel-26* enhancement by selected subunit mutations extends to other subunits of the STRIPAK complex whose mutants also enhanced *mel-26*.

To see how STRIPAK affects katanin's normal meiotic function, we used *mei-2(sb39)*. This *ts* allele has >80% hatching at 15° but has ~2% at 25° (Srayko *et al.* 2000; Beard *et al.* 2016). As MEI-1 interacts with MEI-2 both in vivo and in vitro, genetic interactions with *mei-2* are applicable to *mei-1* (Mains *et al.* 1990a; Clark-Maguire and Mains 1994; Srayko *et al.* 2000; McNally *et al.* 2014; Joly *et al.* 2016). Mutations in *mei-2* result in lethality from failed meiotic spindle formation and abnormal polar body extrusion, leading to lethal aneuploidy. Improper chromosome segregation results in an increase in viable XO males if the only chromosome lost is an X (Hodgkin *et al.* 1979). Thus, the High Incidence of Males (Him) phenotype is an additional readout for meiotic defects that we have often used (Clandinin and Mains 1993; Lu and Mains 2005; Han *et al.* 2009; Johnson *et al.* 2009; Beard *et al.* 2016). The double mutant *mei-2(sb39); hecd-1* decreases hatching for 41% to 8% at 20° compared to *mei-2* alone, while increasing male progeny from 2.2% to 13% (Beard *et al.* 2016). Unless stated otherwise, *sb39* is the allele used in our experiments. The interactions with *mel-26* and *mei-2* we observe are unlikely nonspecific synergy due to phenotypes like alterations in cell division or cytoskeletal defects that are not directly related to katanin. For example, in a previous screen of ~2,500 genes by RNAi for suppression of ectopic katanin function, we found only 1 gene, *ppfr-4*, besides *mei-1* and *mei-2*, indicating that nonspecific genetic interactions are rare (Han *et al.* 2009).

Most STRIPAK core components show the same interaction pattern as *hecd-1*

We first explored STRIPAK genetic interactions during mitosis using double mutants with *mel-26*. Like *hecd-1*, the STRIPAK core components *gck-1*/GCKIII, *farl-11*/Striatin interacting protein, *let-92*/Protein phosphatase 2 and *cash-1*/Striatin enhanced *mel-26* embryonic lethality at 15°. For brood 2, *gck-1(RNAi)* worms had a hatching rate of 80%, while *mel-26* hermaphrodites had a hatching rate of 17%. If *gck-1* lethality was independent of that caused by *mel-26*, the resulting hatching rate would be the product of the control rates (80% × 17%), resulting in a predicted hatching rate of 13%. However, the actual hatching rate of *gck-1(RNAi); mel-26* was 3%, showing more than a 5-times lethality enhancement ($P < 0.0001$, Fig. 2a). This indicates that *gck-1(+)* acts as an inhibitor of katanin function during mitosis (Fig. 1c). Similarly, *farl-11(RNAi); mel-26* showed a 5-times enhancement ($P < 0.0001$, Fig. 2b, Supplementary Fig. 1a; experimental repeats, including at different temperatures or different RNAi broods, are included in Supplementary Figs.). *let-92(RNAi); mel-26* had 3-times increased lethality ($P < 0.0001$, Fig. 2c). *cash-1(RNAi); mel-26* had an enhancement of almost 5-times in brood 2, increasing to 92-fold in brood 3 ($P < 0.0001$ for both broods, Fig. 2d). As we had previously demonstrated for the interaction between *mel-26* and *hecd-1* (Beard *et al.* 2016), *cash-1(RNAi); mel-26* lethality was greatly reduced by the inclusion of the β-tubulin allele *tbb-2(sb26)*, which is partially refractory to katanin severing (Lu *et al.* 2004) ($P < 0.0001$, Fig. 2e). Thus enhancement *mel-26* by STRIPAK mutants likely results from ectopic katanin microtubule severing.

Predicted null alleles of 2 other core STRIPAK components were tested, *mob-4* and *C49H3.6*/CTTNBP2NL. Although statistically significant, these each showed weak interactions with *mel-26* (~1.3-times enhancement) and were not pursued further (Supplementary Fig. 1, b and c).

We next examined STRIPAK genetic interactions during meiosis using double mutants with *mei-2*. The core components *gck-1, farl-11, let-92* and *cash-1* each enhanced *mei-2* at 20°, similar to *hecd-1* (Beard *et al.* 2016). As seen previously with *hecd-1*, interactions were generally weaker than with *mel-26*. *gck-1(RNAi); mei-2* had 46% hatching, while the expected hatching rate was 67%, a 1.5-times increase in lethality at 20° ($P < 0.0001$, Fig. 2f, Supplementary Fig. 1, d and e). This indicates that *gck-1(+)* acts as an activator of katanin function in meiosis (Fig. 1c). *farl-11(RNAi); mei-2* showed a 2.5-times decrease in hatching ($P < 0.0001$, Fig. 2g). Meiotic enhancement was confirmed in *farl-11(RNAi); mei-2* by a 5.6-times increase in male progeny, to 4.6% when the expected was 0.8% ($P < 0.0001$, Fig. 2h, Supplementary Fig. 1, F and G). *let-92(RNAi); mei-2* exhibited a decrease of the hatching rate by 4-times ($P < 0.0001$, Fig. 2l, Supplementary Fig. 1h). Last, *cash-1(RNAi); mei-2* had 2.7-times decrease in hatching ($P < 0.0001$, Fig. 2j, Supplementary Fig. 1i).

These results indicate that the STRIPAK core components *gck-1, farl-11, let-92*, and *cash-1* are interacting with the katanin pathway with the same pattern as *hecd-1*, as an inhibitor of katanin function in mitosis but an activator of katanin function in meiosis (Fig. 1).

ccm-3 behaves differently than other STRIPAK core components

ccm-3 showed a different pattern of interaction with katanin than *hecd-1* and the STRIPAK core components by being an inhibitor at both divisions. Similar to the other STRIPAK core genes, *ccm-3(RNAi)* enhanced *mel-26* lethality, with hatching rate of 0%, compared to the expected rate of 20% at 15° ($P < 0.0001$, Fig. 3a, Supplementary Fig. 2a). To confirm these results, we performed the reciprocal experiment of *mel-26(RNAi)* on the heterozygote

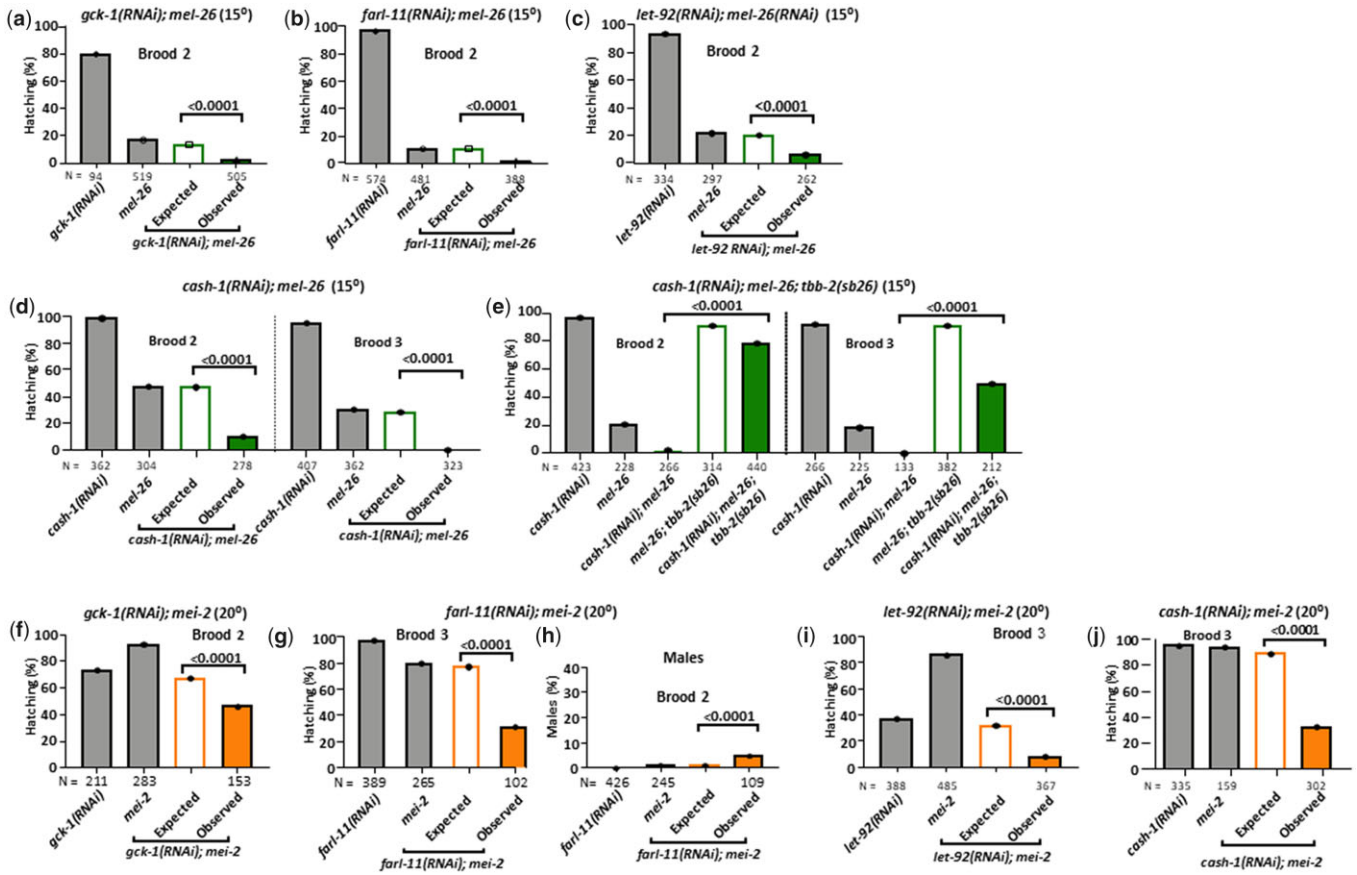

Fig. 2. Genetic interactions of STRIPAK core components with *mel-26* and *mei-2*. White bars are predicted hatching rates based on multiplying the viabilities indicated by the gray bars for the controls run in parallel. Green bars are the observed values of the RNAi knockdowns in the *mel-26(ct61sb4)* background (a–e) or orange for *mei-2(sb39)* (f–j). RNAi broods correspond to plate transfer of parents at the intervals indicated below for each experiment. a) *gck-1(RNAi); mel-26* showed enhancement of lethality with less hatching than predicted. Worms were first exposed to RNAi as L4s, which were transferred at 15° every 2 days to fresh RNAi plates. b) *farl-11(RNAi); mel-26* showed enhancement. L4 worms were exposed to RNAi and transferred every 2 days at 15°. c) *let-92(RNAi); mel-26* showed enhancement. Gravid worms were placed on RNAi plates and transferred at 15° every 12 h. d) *cash-1(RNAi); mel-26* showed enhancement. Young adult worms were fed RNAi at 15° and transferred every day. e) While *cash-1(RNAi); mel-26* showed enhancement of embryonic lethality, this was decreased with the addition of *tbb-2(sb26)*. This allele is partially refractory to katanin microtubule severing, indicating that the increased lethality in *cash-1; mel-26* was due at least in part to ectopic katanin activity. Young adult worms were fed RNAi at 15° and transferred every 12 h. f) *gck-1(RNAi); mei-2* showed enhancement. L3s were exposed to RNAi and transferred at 20° every day. g) *farl-11(RNAi); mei-2* showed enhancement, with a corresponding increase in males (h), an indication of X chromosome nondisjunction giving rise to XO males. L3s were first exposed to RNAi at 20° and transferred daily. i) *let-92(RNAi); mei-2* showed enhancement with decreased hatching. Gravid worms were fed RNAi and transferred at 20° every 4 h. j) *cash-1(RNAi); mei-2* showed decreased hatching. Gravid worms were exposed to RNAi and transferred at 20° every 12 h. *N* = number of progeny for each brood, ≥4 hermaphrodites were used for each genotype. Significance was calculated using a 2-tail binomial test. Additional experiments for these genotypes, leading to the same conclusions, are shown in Supplementary Fig. 1.

ccm-3/mIn1 (*mIn1* is a balancer chromosome). *ccm-3* is homozygous sterile but may sensitize the genetic background as a heterozygote. Enhancement of lethality was again seen at 15°, with more than 3-times decrease in hatching from the 23% expected to 7% ($P < 0.0001$, Fig. 3b). However, *ccm-3* differed from the other tested STRIPAK core genes in that loss of *ccm-3* acted as a suppressor, rather than an enhancer, of *mei-2* lethality. At 23°, *ccm-3(RNAi); mei-2* showed a hatching rate of 51% compared to the expected of 30%, a 1.7-times increase ($P < 0.0001$, Fig. 3c). This result was repeatable in the reciprocal experiment with RNAi of *mei-2* used on the *ccm-3* heterozygote. At 15°, *mei-2(RNAi); ccm-3/mIn1* showed a 3-times rescue ($P < 0.0001$, Fig. 3d, Supplementary Fig. 2b). As expected for a suppressor of meiotic spindle defects that result in nondisjunction, there was a decrease in the fraction of surviving progeny that were male ($P < 0.0001$, Fig. 3e). Finally, the suppression by heterozygous *ccm-3* was also seen using *mei-1(RNAi)* in place of *mei-2(RNAi)* ($P < 0.0001$, Fig. 3f). Thus, *ccm-3* is similar to the other STRIPAK core components and *hecd-1* by enhancing *mel-26* lethality, but *ccm-3* differed by rescuing *mei-2* (and *mei-1*) lethality. This pattern of interaction suggests that *ccm-3* acts as a katanin inhibitor in both meiosis and mitosis (Fig. 1, note that "inhibitor" or "activator" depends on the sum of all genetics interactions between the gene of interest and *mei-2*).

STRIPAK variable components modify interactions with katanin

Unlike the STRIPAK core components, variable component *slmp-1* and *otub-2* mutants display no phenotype of their own. *slmp-1*/Sarcolemma-associated protein, exhibited strong interactions with katanin. The *mel-26; slmp-1* double mutant had a 22% hatching rate at 20°, which represents a more than 20-times suppression compared to the expected hatching rate of 1% ($P < 0.0001$, Fig. 4a, Supplementary Fig. 3a). At 25°, the rescue was at best weak (Fig. 4b), perhaps indicating that *slmp-1* does not modulate a pathway that bypasses *mel-26*. Thus *slmp-1(+)* acts as an activator of ectopic katanin function in mitosis (Fig. 1c).

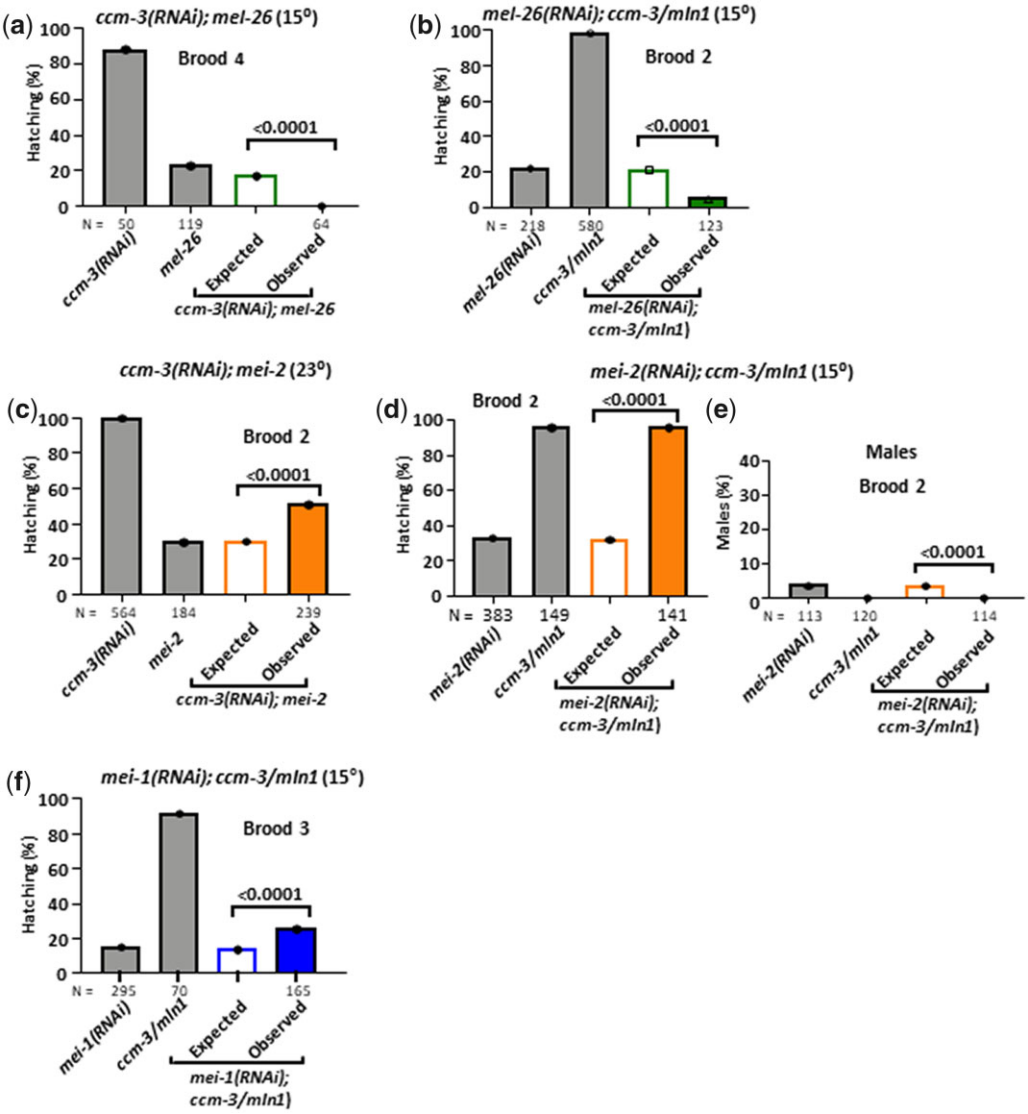

Fig. 3. Genetic interactions of *ccm-3* with the katanin pathway. White bars are predicted hatching rates based on multiplying the viabilities indicated by the gray bars for the controls run in parallel. Green bars are the observed values of mutant or knockdowns in the *mel-26(ct61sb4)* or *mel-26(RNAi)* backgrounds (a,b), orange for *mei-2(sb39)* or *mei-2(RNAi)* c–e), and blue for *mei-1(RNAi)* (f). RNAi broods correspond to plate transfer of parents at the intervals indicated below. a) *ccm-3(RNAi); mel-26* showed enhancement of embryonic lethality beyond what was predicted assuming independence of control viabilities. L4s were first exposed to RNAi and transferred daily to fresh RNAi plates at 15°. b) *mel-26(RNAi); ccm-3/mIn1* showed enhancement. L3s were placed on RNAi at 15° and transferred every 2 days. *mIn1* is a homozygous sterile balancer chromosome marked by *dpy-10*. c) *ccm-3(RNAi); mei-2* showed suppression of embryonic lethality. Gravid adults were exposed to RNAi and transferred at 23° every 12 h. d) *mei-2(RNAi); ccm-3/mIn1* showed suppression with a decrease in males (e), indicating less nondisjunction giving rise to XO males. Gravid adults exposed to RNAi at 15° and were transferred every 12 h. f) *mei-1(RNAi); ccm-3/mIn1* showed suppression. Gravid adults were placed on RNAi at 15° and transferred every 12 h. N = number of progeny, ≥4 hermaphrodites were used for each genotype. Significance was calculated using a 2-tail binomial test. Supporting experiments are included in Supplementary Fig. 2.

slmp-1 also acted as an activator at meiosis, as indicated by *mei-2* enhancement. The hatching rate of *mei-2; slmp-1* at 23° was 11%, compared to 26% in *mei-2* alone, more than 2-times lower than expected ($P < 0.0001$, Fig. 4c, Supplementary Fig. 3b). Incidence of males showed a corresponding 3-fold increase ($P < 0.0001$, Fig. 4d, Supplementary Fig. 3c). Another hypomorphic allele, *mei-2(ct98)* was similar to *mei-2(sb39)* in also showing a decrease of hatching and an increase in males at 25° ($P < 0.0001$ for both, Fig. 4, e and f). When *mei-1* was substituted for *mei-2* using RNAi, the same patterns were observed (Fig. 4, g and h). Overall, these interactions suggest that SLMP-1 acts as an activator in both meiosis and mitosis (Fig. 1c). Kean *et al.* (2011) found that the STRIPAK complex has either C49H3.6/CTTNBP2NL or SLMP-1 present in the complex at 1 time. This is consistent with the result that *slmp-1* showed strong genetical interactions in our system, but *C49H3.6* did not (Supplementary Fig. 1f).

otub-2 encodes a K63 deubiquitinase that could oppose the K63 ubiquitination activity of *hecd-1*. *mel-26 otub-2* at 15° or 18° showed a greater than 2-times rescue ($P < 0.0001$ for both, Fig. 4, l and j, Supplementary Fig. 3d). This is the opposite result of *hecd-1; mel-26* and is expected for a deubiquitinase that antagonizes *hecd-1* ubiquitinase function. In contrast, *otub-2* interactions with *mei-2* were weak and variable (Supplementary Fig. 3, e–k). While we concluded that *otub-2(+)* behaves as a mitotic katanin activator, this gene may have at best a minor role in meiosis.

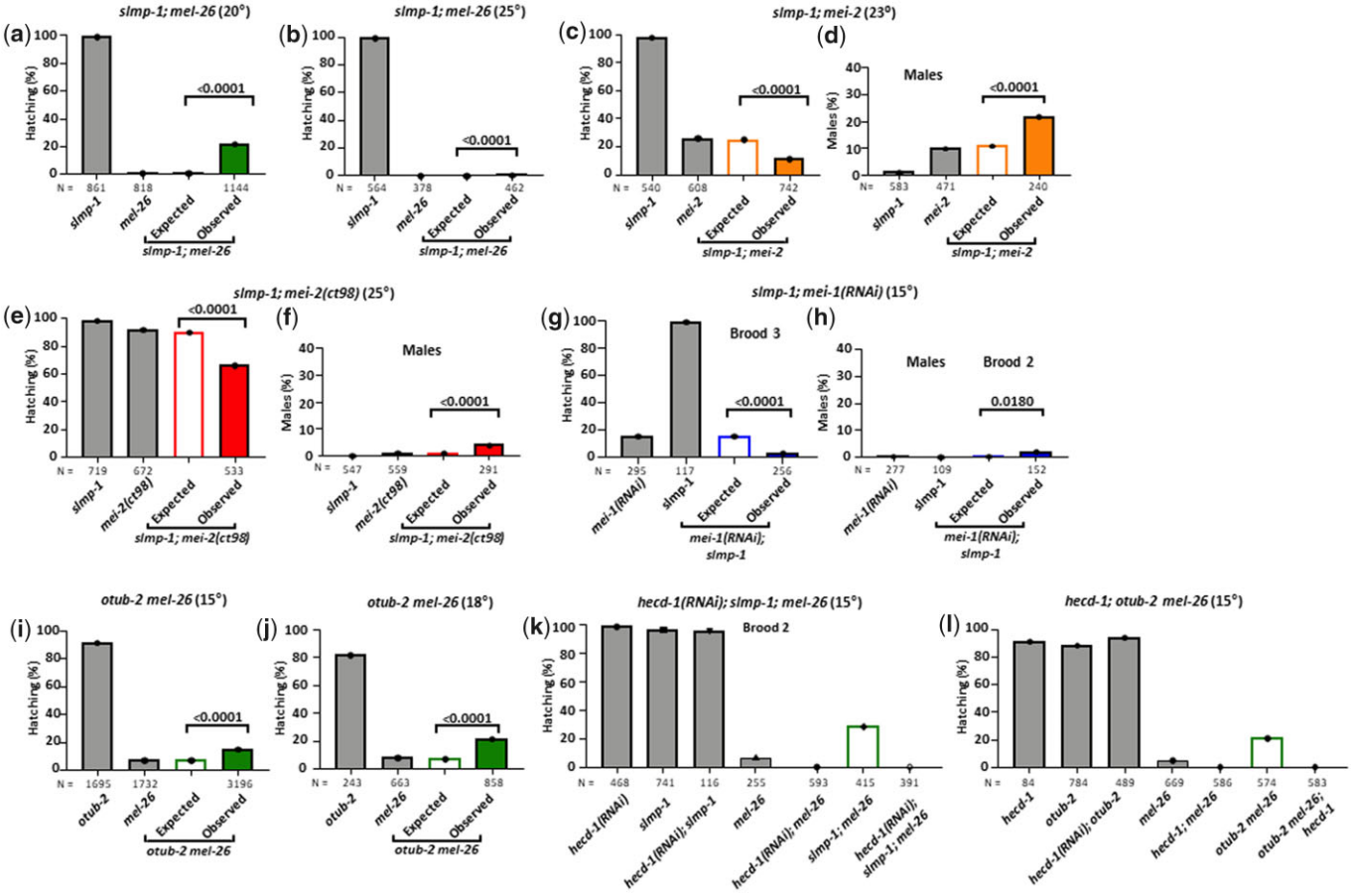

Fig. 4. Genetic interactions of the STRIPAK variable components *slmp-1*, *otub-2*, and *hecd-1* with the katanin pathway. White bars are predicted hatching rates based on multiplying the viabilities indicated by the gray bars for the controls run in parallel. Green bars are the observed values of the mutants in the *mel-26(ct61sb4)* background (a,b,i,j), orange for *mei-2(sb39)* (c,d), red for *mei-2(ct98)* (e,f), and blue for *mei-1(RNAi)* (g,h). RNAi broods correspond to plate transfer of parents at the intervals indicated below. a) *slmp-1; mel-26* showed rescue at 20° but not at 25° (b), indicating that it is unlikely to represent bypass suppression. c) *slmp-1; mei-2(sb39)* showed lethality enhancement and an increase in males as a measure of nondisjunction at 23° (d). e,f) a second hypomorphic *mei-2* allele, *ct98*, showed the same pattern with *slmp-1* at 25°. g,h) *slmp-1; mei-1(RNAi)* showed enhancement with increased male progeny. Gravid adults were exposed to RNAi at 15°and transferred every 12 h. *otub-2 mel-26* showed rescue of embryonic lethality at 15° (i) and 18° (j). k) *hecd-1(RNAi) slmp-1; mel-26* showed the same low hatching rate as did *hecd-1(RNAi); mel-26* rather than the suppression of *slmp-2; mel-26*, suggesting *hecd-1* is downstream of *slmp-1*. L3s were first exposed to RNAi at 15° and transferred every 2 days. l) *hecd-1(RNAi); otub-2 mel-26* showed that enhancement by *hecd-1* is epistatic to suppression by *otub-2*, suggesting *hecd-1* functions downstream of *otub-2*. L3s were placed on RNAi at 15° and transferred every 2 days. N = number of progeny, ≥4 hermaphrodites were used for each genotype. Significance was calculated using a 2-tail binomial test. Supporting data are presented in Supplementary Fig. 3.

otub-2 and *slmp-1* are upstream of *hecd-1* in mitosis

hecd-1 and most STRIPAK core components enhanced the lethality of ectopic katanin function in a *mel-26* background, but variable components, *slmp-1* and *otub-2*, suppressed it. Therefore, triple mutants containing *mel-26* and *hecd-1* with either *slmp-1* or *otub-2* can be used to determine the gene order in the pathway. For 2 genes acting in opposition, elimination of both results in the phenotype of the downstream gene. *hecd-1(RNAi); mel-26* showed enhancement with no hatching at 15° while *slmp-1; mel-26* showed rescue with 33% hatching, which was above the control value of 6% (Fig. 4k). No hatching was seen in the *hecd-1(RNAi); slmp-1; mel-26* triple mutant. Thus suppression of *mel-26* by loss of *slmp-1* requires *hecd-1(+)* activity, that is *slmp-1* mutants result in altered HECD-1 activity. Similarly, there was no hatching in the *hecd-1; otub-2 mel-26* strain, again showing that *hecd-1* enhancement is epistatic to *otub-2* suppression (Figure 4l, Supplementary Fig. 3n). This result is expect if the HECD-1 and OTUB-2 act on the same substrate—loss of the OTUB-2 deubiquitinase leads to increased net ubiquitination, but only when the HECD-1 ubiquitinase is present. Thus *hecd-1* is genetically downstream of both *slmp-1* and *otub-2* (Fig. 1a).

Possible intermediators between STRIPAK/HECD-1 and katanin

We explored several candidates that could serve as a link between HECD-1 and STRIPAK to katanin. SLMP-1 physically interacts with the *C. elegans* kinesin ZEN-4 (Mutlu *et al.* 2018). The *Drosophila* ZEN-4 homolog Subito acts in the augmin pathway to nucleate microtubules in meiosis and mitosis by recruiting γ-tubulin (Bennabi *et al.* 2016; Romé and Ohkura 2018) and γ-tubulin acts in parallel to *C. elegans* katanin to nucleate meiotic spindles (McNally *et al.* 2006). ZEN-4 is also part of the centralspindlin complex, which is involved in *C. elegans* polar body formation (Schlientz and Bowerman 2020).

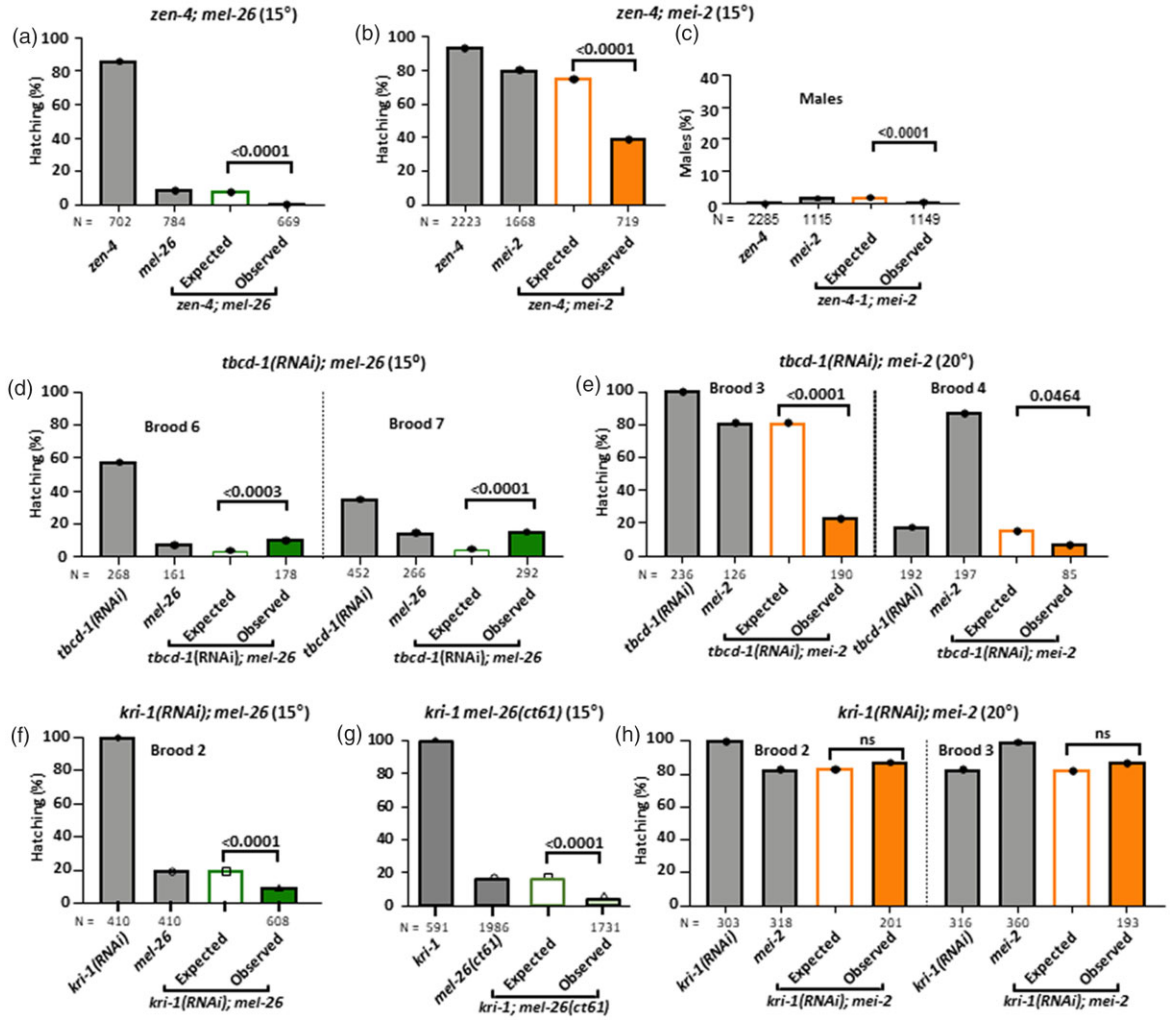

Fig. 5. Interaction of *zen-4*, *tbcd-1*, and *kri-1* with katanin pathway mutants. White bars are predicted hatching rates based on multiplying the viabilities indicated by the gray bars for the controls run in parallel. Green bars are the observed values with *mel-26* mutants (a,d,f,g) or orange for *mei-2(sb39)* (b,c,e,h). RNAi broods correspond to plate transfer of parents at the intervals indicated below. a) *zen-4; mel-26* showed enhancement of lethality at 15°. b) *zen-4; mei-2* at 20° showed lethality enhancement without an increase in males (c). d) *tbcd-1(RNAi); mel-26* rescued embryonic lethality. Animals were exposed to RNAi as L4s at 15° and transferred every 12 h. e) *tbcd-1(RNAi); mei-2* showed enhancement. Gravid adults were placed on RNAi at 20° and transferred every 12 h. f) *kri-1(RNAi); mel-26(ct61sb4)* enhanced embryonic lethality. L3s were exposed to RNAi at 15° and transferred every 2 days. g) *kir-1 mel-26(ct61)* also showed enhancement. *ct61* is a dominant-negative allele while *ct61sb4* is a null. (H) *kri-1(RNAi); mei-2* showed no interaction in 2 broods. Hermaphrodites were exposed to RNAi at 20° as L3s and transferred every day. *N* = number of progeny, ≥4 hermaphrodites were used for each genotype. Significance was calculated using a 2-tail binomial test. Supporting data are included in Supplementary Fig. 4.

Experiments with a *ts* allele of *zen-4* with *mel-26* and *mei-2* both showed an enhancement of lethality. In mitosis, *zen-4; mel-26* showed an enhancement of more than 13-times at 15° (Fig. 5a). In meiosis, *zen-4; mei-2* showed an enhancement of almost 2-times at 25° and over 3-times at 20° ($P < 0.0001$ for both, Fig. 5b, Supplementary Fig. 4a). Thus *zen-4(+)* acts as an activator of meiotic katanin and an inhibitor of mitotic katanin, similar to *hecd-1* and STRIPAK core components (Fig. 1). Curiously, even though *zen-4* exacerbates the meiotic lethality, there was a decrease, rather than the expected increase, in males in *zen-4; mei-2* ($P < 0.0001$, Fig. 5c, Supplementary Fig. 4b). Among 1149 surviving progeny of *zen-4; mei-2* we expected 23 males, but we found only 5. This indicates that while ZEN-4 acts as activator of meiotic katanin, it may act differently than the STRIPAK and HECD-1 (see *Discussion*).

TBCD-1 is a tubulin chaperone that maintains the pool of tubulin dimers and the homologs of TBCD-1 and *farl-11* interact in *Drosophila* (Nithianantham *et al.* 2015; Sakuma *et al.* 2015). *tbcd-1(RNAi)* resulted in a 2-3 fold rescue of *mel-26* at 15° ($P < 0.0003$, Fig. 5d, Supplementary Fig. 4c). *tbcd-1(RNAi)* caused a 2–4-times enhancement of meiotic lethality in *mei-2* ($P < 0.0001$ and $P = 0.0464$ in broods 3 and 4, respectively, Fig. 5e). These results suggest that TBCD-1 activates katanin function at both divisions (Fig. 1).

kri-1 shows synthetic lethality with *ccm-3* in *C. elegans* (Lant *et al.* 2015). At 15°, *kri-1(RNAi)* in a *mel-26* background showed a 2-times enhancement ($P < 0.0001$, Fig. 5f). A 4-times enhancement was seen using a *kri-1* mutant and the dominant-negative allele *mel-26(ct61)* ($P < 0.0001$, Fig. 5g). Thus like *ccm-3* (Fig. 3, a and b), *kri-1(+)* acts as an inhibitor of mitotic katanin. However, no genetic interactions were observed in *kri-1(RNAi)* and *mei-2* (Fig. 5h).

HECD-1 is ubiquitously expressed in the embryo

To determine the location of HECD-1, in particular to see if it colocalizes with katanin or is found in the meiotic or mitotic spindles, we created a CRISPR N-terminal FLAG-tagged HECD-1

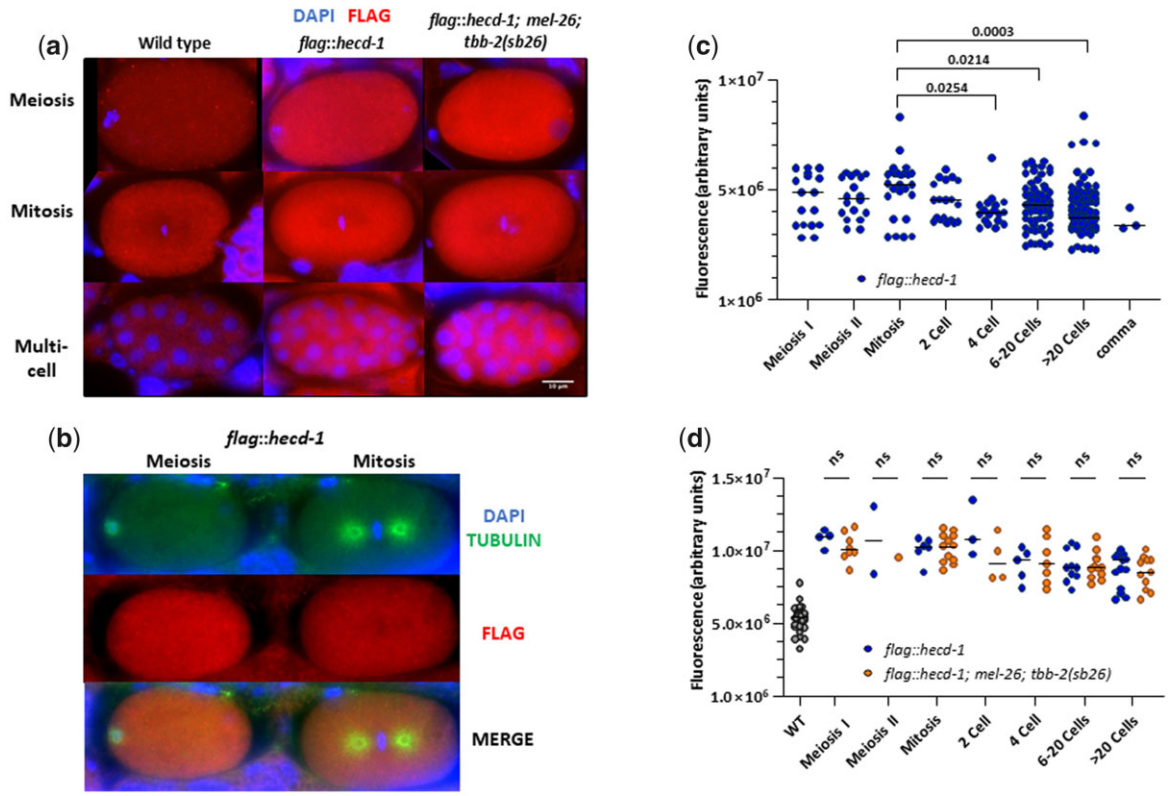

Fig. 6. HECD-1::FLAG embryonic expression. a) Anti-FLAG (red) and DAPI (blue) staining of wild-type and *flag::hecd-1* embryos. Low staining in wild-type compared to *flag::hecd-1*shows the specificity of anti-FLAG (left column, quantified in d). Embryos had ubiquitous FLAG::HECD-1 localization in the cytoplasm, but this was absent from the nucleus at all stages (middle column, unmerged images are presented in Supplementary Fig. 5). No change in localization was apparent between meiosis and mitosis. FLAG::HECD-1 levels were not increased in the *mel-26* background (right column). *tbb-2(sb26)* decreases katanin microtubule severing and was included to restore normal morphology so that embryos could be compared. Exposure times were the same in all embryos. Controls were stained on the same slide as the transgenics. Scale bar = 10 μm. b) Adjacent meiotic (left) and mitotic (right) embryos on the same slide showed no apparent colocalization of anti-FLAG (red) with anti-tubulin (green) and DAPI (blue) staining. c) Quantification of anti-FLAG staining in the *flag::hecd-1* background. There was no change FLAG::HECD-1 levels from meiosis to mitosis, although there was a slight decrease at later stages. One-way ANOVA was used to compare stages. d) Quantification of FLAG::HECD-1 levels in the *mel-26* background. Levels at the same embryonic stage did not vary between the *flag::hecd-1* and *flag::hecd-1*; *mel-26* backgrounds. Low staining in the wildtype compared to *flag::hecd-1* shows the specificity of anti-FLAG. Unpaired t-tests were used to calculate the significance between 2 strains in the same stage. Supporting data can be found in Supplementary Fig. 5.

allele, *sb142*. This allele retains wild-type function in that unlike *hecd-1* mutants, *flag::hecd-1* did not enhance *mel-26* lethality (Supplementary Fig. 5a). Using a fluorescent anti-FLAG antibody in fixed embryos, expression of HECD-1 was ubiquitous in the cytoplasm of the developing embryo, but was absent from the nucleus (Fig. 6a, Supplementary Fig. 5b). We could detect no obvious colocalization of FLAG::HECD-1 with either meiotic or mitotic microtubules (Fig. 6b). These patterns were consistent through later stages of development, although levels gradually decreased over time (Fig. 6c). Importantly, no changes were apparent between meiosis and mitosis.

Gomes *et al.* (2013) showed HECD-1 interacted with MEL-26 in a yeast 2-hybrid screen. As an adaptor protein for the CUL-3 ubiquitin ligase, MEL-26 might degrade HECD-1 as it does for 2 other proteins the authors found in their screen, MEI-1 and PPFR-1. Because *mel-26* results in embryos with aberrant cell division, we included the *tbb-2(sb26)* allele that is partially resistant to katanin severing (Lu *et al.* 2004) to restore normal embryo morphology to the strain. Comparisons of FLAG::HECD-1 expression in the wild-type background and the *mel-26; tbb-2(sb26)* background showed no significant differences in expression at any stage of development (Fig. 6, a and d). In addition, FLAG::HECD-1 levels were consistent between zygotes with either properly formed spindles in embryos rescued by *tbb-2(sb26)* and their siblings that had abnormal morphology (Supplementary Fig. 5c). These results suggest that HECD-1 is not a target of MEL-26 for degradation.

Discussion

After the completion of meiosis in the *C. elegans* embryo, katanin microtubule severing is downregulated to ensure successful formation of the mitotic spindle in the same cytoplasm, in less than 15 min. We previously found that 2 ubiquitin ligases (CUL-2 and CUL-3) act in parallel for MEI-1 degradation, while a third ubiquitin ligase (HECD-1) acts independently of degradation (Lu and Mains 2007; Beard *et al.* 2016). Here, we report that the evolutionarily conserved STRIPAK complex genetically interacts with *hecd-1* and katanin (Fig. 1). The STRIPAK complex is involved in many developmental and cellular processes from fungi to mammals, including WNT, JNK, and Hippo signaling, cell migration, apoptosis, endocytosis, membranous tubule formation, and cardiovascular development (Hwang and Pallas 2014; Shi *et al.* 2016; Kuck *et al.* 2019; Kuck and Stein 2021). Perhaps our most interesting findings are that STRIPAK regulates katanin differently in meiosis and mitosis and that the variable components (*otub-2, slmp-1*)

could be responsible for these differences. A major question is how STRIPAK can be involved in many diverse, and seemingly unrelated, processes in *C. elegans* as well as in other organisms. We suggest that differing subunit composition can cause significant differences in STRIPAK function.

STRIPAK components regulate microtubule severing

hecd-1 switches from being a meiotic activator to a mitotic inhibitor of katanin. The basis for this is unknown, but perhaps HECD-1 biases katanin toward favoring meiotic microtubules (and hence is a meiotic activator) over mitotic microtubules (and so functions as an inhibitor in mitosis). We will first discuss genetic interactions of STRIPAK components with katanin during mitosis, which like *hecd-1* (Beard *et al.* 2016), are generally stronger than those in meiosis.

The genes for the STIPAK core components *let-92, farl-11, cash-1, ccm-3*, and *gck-1* enhanced *mel-26* embryonic lethality (Fig. 2). Enhanced lethality of *mel-26* by *cash-1* and *hecd-1* were suppressed by addition of the *tbb-2(sb26)* mutation, which is partially resistant to katanin microtubule severing. This indicates that lethality was caused by katanin misregulation (Lu *et al.* 2004). We suggest that enhancement of *mel-26* by the other STRIPAK subunits we tested indicates that they are in the same complex as CASH-1 and HECD-1 and are also affecting katanin. Thus STRIPAK core components formally behaved as genetic inhibitors of katanin function in mitosis (Fig. 1). The variable components *otub-2* and *slmp-1* instead acted as activators of mitotic katanin activity as their loss rescued *mel-26* lethality (Fig. 4), implying that the 2 genes oppose *hecd-1* and core STRIPAK functions. Based on the biochemical properties of their mammalian homologs (Tran *et al.* 2013), the deubiquitinase activity of OTUB-2 would antagonize HECD-1 ubiquitination. This implies they may share substrates, and indeed the epistasis of *hecd-1* over *otub-2* is consistent with this idea in that the suppression of *mel-26* lethality by removal of *otub-2* ubiquitinase results in more net ubiquitination that is dependent on *hecd-1(+)* (Fig. 4). Similarly, addition of the SLMP-1 subunit to the STRIPAK core may alter its function such that STRIPAK can no longer activate HECD-1. It will be interesting to see if these variable components act similarly in other organisms to alter STRIPAK function. Similar to the work of Lant *et al.* (2015) on *C. elegans* excretory cell extension, *mob-4* and *C49H3.6*/CTTNBP2NL had little to no interaction in katanin regulation.

Turning to meiosis, the core components *let-92, farl-11, cash-1*, and *gck-1* behaved similar to *hecd-1* as genetic activators of katanin function—loss led to increased lethality in conjunction with hypomorphic alleles of *mei-2* (Fig. 2). The observed increase in males in *farl-11* and *slmp-1* [and previously for *hecd-1* (Beard *et al.* 2016)] confirmed that lethality stemmed from meiotic defects that led to chromosome nondisjunction, namely the Him phenotype. Consistent with the idea that the meiotic spindle is the relevant target, *ccm-3*, which rescued rather than enhanced *mei-2* lethality, resulted in a corresponding decrease rather than an increase in males. We suggest that defects in the meiotic spindle, as inferred by the Him phenotype, are also true of the other mutant STRIPAK subunits that enhanced *mei-2* lethality. Unlike the case in mitosis where *slmp-1* and *hecd-1* showed opposite interactions with *mei-2*, mutations of the variable STRIPAK component *slmp-1* showed meiotic phenotypes similar to *hecd-1* and STRIPAK core genes (interactions of *otub-2* with *mei-2* were inconsistent).

Although *ccm-3* was similar to other core components during mitosis, it differed from all genes that we tested in strongly suppressing, rather than enhancing, *mei-2* (Fig. 3). Genetic interactions in both meiosis and mitosis were strong, even when *ccm-3* was heterozygous. A possible explanation for the difference between *ccm-3* and the other STRIPAK core components in mitosis is that STRIPAK lacking CCM-3 may have neomorphic properties. For example, since CCM-3 recruits GCK-1 (Kuck *et al.* 2019; Bae *et al.* 2020), STRIPAK without both CCM-3 and GCK-1 (in a *ccm-3* mutant) could act differently than in absence of GCK-1 alone (in a *gck-1* mutant). By contrast, *gck-1* and *ccm-3* have similar phenotypes in *C. elegans* for formation of the excretory canal, germline, and in vesicle trafficking (Lant *et al.* 2015; Pal *et al.* 2017). Differences with these activities and katanin regulation may demonstrate STRIPAK has different functions in different processes. CCM-3 has STRIPAK-independent functions (Lant *et al.* 2015), which could also contribute to the differences.

HECD-1 embryonic localization

To gain insight in how HECD-1 influenced katanin function, we examined HECD-1 expression in the embryo using a functional FLAG-tagged allele. One hypothesis was that HECD-1 localizes to the spindle where it could influence MEI-1 activity and this might change during the meiosis to mitosis transition. However, embryonic FLAG::HECD-1 had ubiquitous cytosolic expression, including during both meiosis and mitosis, with no detectible enrichment on microtubules (Fig. 6). MEL-26, a substrate adaptor for CUL-3 ubiquitin ligase, binds HECD-1, MEI-1 and PPFR-1 in yeast 2-hybrid assays (Gomes *et al.* 2013). We asked if HECD-1 could be a target of MEL-26 mediated proteosomal degradation as it does for MEI-1 and PPFR-1. However, we found no changes for FLAG::HECD-1 in the *mel-26* background (Fig. 6).

As HECD-1 is proposed to ubiquitinate its substrates through K63 linkages, staining with an K63 antibody could reveal where HECD-1 substrates might be localized. There was no apparent K63 staining in the meiotic or mitotic spindles in the images presented by Hajjar *et al.* (2014) or Sato *et al.* (2014). K63 was found on the membranous organelles contributed by the sperm (Hajjar *et al.* 2014), but we found no enrichment of our FLAG::HECD-1 in that region (Fig. 6). Sato *et al.* (2014) saw K63 staining in the cortical puncta in meiosis II. Interestingly the katanin inhibitor MBK-2 is found at the cortex at this time along with the MBK-2 regulators EGG-3 and CHS-1 (Maruyama *et al.* 2007; Stitzel *et al.* 2007; Sato *et al.* 2014). While MBK-2, unlike HECD-1, does contribute to MEI-1 degradation (Pellettieri *et al.* 2003; Quintin *et al.* 2003; Beard *et al.* 2016), MBK-2 has an additional role in regulating katanin at the level of enzymatic activity (Joly *et al.* 2020). Thus MBK-2, EGG-3, and CHS-1 are potential HECD-1 targets.

Genes providing possible links between STRIPAK and katanin

Expression pattern of FLAG::HECD-1 did not reveal insights into how it might influence katanin, and so STRIPAK interactions could be indirect. Therefore, we looked at other genes known to physically interact with STRIPAK and the microtubule cytoskeleton that might mediate our observed genetic interactions. Sakuma *et al.* (2015) showed that Strip (*farl-11*) physically and genetically interacts with TBCD/tubulin cofactor D and binds to *Drosophila* microtubules. Human TBCD has roles in centriole formation and spindle organization and localizes to the chromosomes in meiosis (Fanarraga *et al.* 2010; Jimenez-Moreno and Agirregoitia 2017). In *C. elegans, tbcd-1* RNAi results in weak mitotic defects similar to *mel-26* (Gerson-Gurwitz *et al.* 2016), so a *mel-26* enhancement would be expected. Surprisingly, a rescue was seen indicating that *tbcd-1* loss may stabilize microtubules against katanin severing (Fig. 5). Likewise, *tbcd-1* knockdown enhanced the *mei-2* hypomorph,

indicating that again microtubules could be less susceptible to katanin. TBCD-1 has a dual role in both folding and unfolding tubulin heterodimers (Nithianantham *et al.* 2015). Perhaps RNAi was selectively affecting the unfolding function, or the folding function is redundant with other factors. Either situation could result in an increase in pools of tubulin heterodimers and a net stabilization of microtubules against katanin severing.

ZEN-4 may also provide a link between STRIPAK and katanin function. *Caenorhabditis elegans* ZEN-4 physically interacts with SLMP-1 (Mutlu *et al.* 2018). *zen-4* encodes a kinesin-6 protein; this family of proteins help nucleate acentrosomal microtubules in mitosis and meiosis with augmin, which recruits the γ-tubulin ring complex to nucleate microtubules (Romé and Ohkura 2018). γ-tubulin acts in parallel to katanin during meiotic spindle formation and becomes essential for this process only in a katanin loss of function mutant (McNally *et al.* 2006). If STRIPAK acts with γ-tubulin in parallel to katanin, this would explain the lack of obvious phenotypes in STRIPAK mutants on their own but enhancement when coupled with *mei-2* hypermorphic mutations.

A nonmutually exclusive model for genetic interactions between *zen-4* and katanin is suggested by the unexpected observation that while *zen-4* resembled *hecd-1* and all STRIPAK mutants in enhancing *mei-2* meiotic lethality, it did so without a concomitant increase in males (Fig. 5). We assumed that enhancement of lethality stems directly from defects in meiotic spindle formation and the associated nondisjunction and aneuploidy. However, abnormal polar body formation is another phenotype seen when katanin is limiting, in *mei-1* or *mei-2* mutants (Mains *et al.* 1990a), with loss of the katanin activator *ppfr-1* (Han *et al.* 2009; Gomes *et al.* 2013) or with tubulin mutants that are refractory to katanin severing (Lu and Mains 2005). While abnormal spindle formation can lead to subsequent polar body defects, here we speculate that an independent function of katanin during polar body formation enhances meiotic lethality without increasing nondisjunction. Homologs of ZEN-4 have cytokinetic defects as part of the centralspindlin complex, which is involved in contractile ring formation, including during *C. elegans* polar body formation (Raich *et al.* 1998; Fabritius *et al.* 2011; Schlientz and Bowerman 2020). Furthermore, katanin function is required at meiosis II for polar body abscission (Gomes *et al.* 2013). If katanin and *zen-4* mutations specifically enhance polar body cytokinetic defects, this could lead to missegregation of all chromosomes at once (lethal aneuploidy) rather than the single chromosome loss seen with spindle abnormalities that can give rise to XO males. Thus *zen-4* would enhance *mei-2* lethality without an increase in males.

A similar model proposing a role in cytokinesis could apply to the enhancement of *mel-26* lethality by *zen-4* or STRIPAK mutants during mitosis. It is clear that significant mitotic lethality does stem from ectopic katanin severing during mitosis [i.e. *mel-26* suppression by *tbb-2(sb26)* shows that katanin severing is involved, Fig. 2]. However, a role of STRIPAK and *mel-26* is possible in cell abscission, which could independently contribute to the lethality. Mitotic phenotypes in *mel-26* mutants include cytokinesis defects, which result in ectopic furrow formation (Mains *et al.* 1990a; Luke-Glaser *et al.* 2005). Pal *et al.* (2017) observed STRIPAK components localize to cleavage furrows of germ cells and embryos.

How the evolutionary conserved STRIPAK complex has been adapted to a wide variety of dissimilar processes is a major question. Our work tested the functions of 10 STIRPAK components in a single multicellular organism, demonstrating that different subunits have different functions, and that STRIPAK functions differ with time as the oocyte transitions from meiosis to mitosis. While we have candidate genes that bridge STRIPAK and HECD-1 to katanin function, underlying mechanisms needs further study. These may reveal further intricacies of MEI-1/MEI-2 regulation, which includes multiple levels of redundancy, and how STRIPAK functions can be adapted for its meiotic vs. mitotic functions. This complexity reflects the precise temporal control that is required to restrict the potent, and potentially dangerous, katanin microtubule-severing function to the narrow meiotic temporal window.

Data availability

Strains and plasmids are available upon request. The authors affirm that all data necessary for confirming the conclusions of the article are present within the article, figures, and tables.

Supplemental material is available at *GENETICS* online.

Acknowledgments

The authors would like to thank the members of the MCGHEE, HANSEN, and TARAILO-GRAOVAC labs for suggestions throughout this project and J. Mcghee and F. Snider for technical advice. W.B. Derry, B. Lant, and J. Guo provided strains and reagents. We also thank Wormbase.

Funding

This work was supported by the Natural Science and Engineering Council of Canada (NSERC, RGPIN-2017-04132) to PEM. Some strains were provided by the CGC, which is funded by NIH Office of Research Infrastructure Programs (P40 OD010440).

Conflicts of interest

None declared.

Literature cited

Akutsu M, Dikic I, Bremm A. Ubiquitin chain diversity at a glance. J Cell Sci. 2016;129:875–880.

Baas PW, Rao AN, Matamoros AJ, Leo L. Stability properties of neuronal microtubules. Cytoskeleton (Hoboken). 2016;73(9):442–460.

Bae SJ, Ni L, Luo X. STK25 suppresses Hippo signaling by regulating SAV1-STRIPAK antagonism. eLife. 2020;9:e54863.

Bai SW, Herrera-Abreu MT, Rohn JL, Racine V, Tajadura V, Suryavanshi N, Bechtel S, Wiemann S, Baum B, Ridley AJ, *et al.* Identification and characterization of a set of conserved and new regulators of cytoskeletal organization, cell morphology and migration. BMC Biol. 2011;9:54.

Beard SM, Smit RB, Chan BG, Mains PE. Regulation of the MEI-1/MEI-2 microtubule-severing katanin complex in early *Caenorhabditis elegans* development. G3 (Bethesda). 2016;6(10):3257–3268.

Bel Borja L, Soubigou F, Taylor SJP, Fraguas Bringas C, Budrewicz J, Lara-Gonzalez P, Sorensen Turpin CG, Bembenek JN, Cheerambathur DK, Pelisch F, *et al.* BUB-1 targets PP2A: b 56 to regulate chromosome congression during meiosis I in *C. elegans* oocytes. eLife. 2020;9:e65307.

Bennabi I, Terret ME, Verlhac MH. Meiotic spindle assembly and chromosome segregation in oocytes. J Cell Biol. 2016;215(5):611–619.

Brenner S. The genetics of *Caenorhabditis elegans*. Genetics. 1974;77(1):71–94.

Clandinin TR, Mains PE. Genetic studies of *mei-1* gene activity during the transition from meiosis to mitosis in *Caenorhabditis elegans*. Genetics. 1993;134(1):199–210.

Clark-Maguire S, Mains PE. Localization of the *mei-1* gene product of *Caenorhabditis elegans*, a meiotic-specific spindle component. J Cell Biol. 1994;126(1):199–209.

Connolly AA, Osterberg V, Christensen S, Price M, Lu C, Chicas-Cruz K, Lockery S, Mains PE, Bowerman B. *Caenorhabditis elegans* oocyte meiotic spindle pole assembly requires microtubule severing and the calponin homology domain protein ASPM-1. Mol Biol Cell. 2014;25(8):1298–1311.

Dow MR, Mains PE. Genetic and molecular characterization of the *Caenorhabditis elegans* gene, *mel-26*, a postmeiotic negative regulator of *mei-1*, a meiotic-specific spindle component. Genetics. 1998;150(1):119–128.

Elramli N, Karahoda B, Sarikaya-Bayram Ö, Frawley D, Ulas M, Oakley CE, Oakley BR, Seiler S, Bayram Ö. Assembly of a heptameric STRIPAK complex is required for coordination of light-dependent multicellular fungal development with secondary metabolism in *Aspergillus nidulans*. PLoS Genet. 2019;15(3):e1008053.

Fabritius AS, Flynn JR, McNally FJ. Initial diameter of the polar body contractile ring is minimized by the centralspindlin complex. Dev Biol. 2011;359(1):137–148.

Fanarraga ML, Bellido J, Jaen C, Villegas JC, Zabala JC. TBCD links centriologenesis, spindle microtubule dynamics, and midbody abscission in human cells. PLoS One. 2010;5(1):e8846.

Frost A, Elgort MG, Brandman O, Ives C, Collins SR, Miller-Vedam L, Weibezahn J, Hein MY, Poser I, Mann M, *et al.* Functional repurposing revealed by comparing *S. pombe* and *S. cerevisiae* genetic interactions. Cell. 2012;149(6):1339–1352.

Fu W, Wu H, Cheng Z, Huang S, Rao H. The role of katanin p60 in breast cancer bone metastasis. Oncol Lett. 2018;15(4):4963–4969.

Furukawa M, He YJ, Borchers C, Xiong Y. Targeting of protein ubiquitination by BTB-Cullin 3-Roc1 ubiquitin ligases. Nat Cell Biol. 2003;5(11):1001–1007.

Gerson-Gurwitz A, Wang S, Sathe S, Green R, Yeo GW, Oegema K, Desai A. A small RNA-catalytic argonaute pathway tunes Germline transcript levels to ensure embryonic divisions. Cell. 2016;165(2):396–409.

Gomes J-E, Tavernier N, Richaudeau B, Formstecher E, Boulin T, Mains PE, Dumont J, Pintard L. Microtubule severing by the katanin complex is activated by PPFR-1-dependent MEI-1 dephosphorylation. J Cell Biol. 2013;202(3):431–439.

Goudreault M, D'Ambrosio LM, Kean MJ, Mullin MJ, Larsen BG, Sanchez A, Chaudhry S, Chen GI, Sicheri F, Nesvizhskii AI, *et al.* A PP2A phosphatase high density interaction network identifies a novel striatin-interacting phosphatase and kinase complex linked to the cerebral cavernous malformation 3 (CCM3) protein. Mol Cell Proteomics. 2009;8(1):157–171.

Hajjar C, Sampuda KM, Boyd L. Dual roles for ubiquitination in the processing of sperm organelles after fertilization. BMC Dev Biol. 2014;14:6.

Han X, Gomes J-E, Birmingham CL, Pintard L, Sugimoto A, Mains PE. The role of protein phosphatase 4 in regulating microtubule severing in the *Caenorhabditis elegans* embryo. Genetics. 2009;181(3):933–943.

Hodgkin J, Horvitz HR, Brenner S. Nondisjunction mutants of the nematode *Caenorhabditis elegans*. Genetics. 1979;91(1):67–94.

Hu WF, Pomp O, Ben-Omran T, Kodani A, Henke K, Mochida GH, Yu TW, Woodworth MB, Bonnard C, Raj GS, *et al.* Katanin p80 regulates human cortical development by limiting centriole and cilia number. Neuron. 2014;84(6):1240–1257.

Hwang J, Pallas DC. STRIPAK complexes: structure, biological function, and involvement in human diseases. Int J Biochem Cell Biol. 2014;47:118–148.

Jimenez-Moreno V, Agirregoitia E. Expression and localization of tubulin cofactors TBCD and TBCE in human gametes. Zygote. 2017;25(3):304–312.

Johnson J-LFA, Lu C, Raharjo E, McNally K, McNally FJ, Mains PE. Levels of the ubiquitin ligase substrate adaptor MEL-26 are inversely correlated with MEI-1/katanin microtubule-severing activity during both meiosis and mitosis. Dev Biol. 2009;330(2):349–357.

Joly N, Beaumale E, Van Hove L, Martino L, Pintard L. Phosphorylation of the microtubule-severing AAA+ enzyme Katanin regulates *C. elegans* embryo development. J Cell Biol. 2020;219:e201912037.

Joly N, Martino L, Gigant E, Dumont J, Pintard L. Microtubule-severing activity of the AAA+ ATPase Katanin is essential for female meiotic spindle assembly. Development. 2016;143(19):3604–3614.

Kamath RS, Ahringer J. Genome-wide RNAi screening in *Caenorhabditis elegans*. Methods. 2003;30(4):313–321.

Karabay A, Yu W, Solowska JM, Baird DH, Baas PW. Axonal growth is sensitive to the levels of katanin, a protein that severs microtubules. J Neurosci. 2004;24(25):5778–5788.

Kean MJ, Ceccarelli DF, Goudreault M, Sanches M, Tate S, Larsen B, Gibson LCD, Derry WB, Scott IC, Pelletier L, *et al.* Structure-function analysis of core STRIPAK Proteins: a signaling complex implicated in Golgi polarization. J Biol Chem. 2011;286(28):25065–25075.

Kuck U, Radchenko D, Teichert I. STRIPAK, a highly conserved signaling complex, controls multiple eukaryotic cellular and developmental processes and is linked with human diseases. Biol Chem. 2019;400(8):1005–1022.

Kuck U, Stein V. STRIPAK, a key regulator of fungal development, operates as a multifunctional signaling hub. J Fungi (Basel). 2021;7:443.

Lant B, Yu B, Goudreault M, Holmyard D, Knight JDR, Xu P, Zhao L, Chin K, Wallace E, Zhen M, *et al.* CCM-3/STRIPAK promotes seamless tube extension through endocytic recycling. Nat Commun. 2015;6:6449.

Loughlin R, Wilbur JD, McNally FJ, Nedelec FJ, Heald R. Katanin contributes to interspecies spindle length scaling in *Xenopus*. Cell. 2011;147(6):1397–1407.

Lu C, Mains PE. Mutations of a redundant α-tubulin gene affect *Caenorhabditis elegans* early embryonic cleavage via MEI-1/Katanin-dependent and -independent pathways. Genetics. 2005;170(1):115–126.

Lu C, Mains PE. The *C. elegans* anaphase promoting complex and MBK-2/DYRK kinase act redundantly with CUL-3/MEL-26 ubiquitin ligase to degrade MEI-1 microtubule-severing activity after meiosis. Dev Biol. 2007;302(2):438–447.

Lu C, Srayko M, Mains PE. The *Caenorhabditis elegans* microtubule-severing complex MEI-1/MEI-2 katanin Interacts differently with two superficially redundant beta-tubulin isotypes. Mol Biol Cell. 2004;15(1):142–150.

Luke-Glaser S, Pintard L, Lu C, Mains PE, Peter M. The BTB protein MEL-26 promotes cytokinesis in *C. elegans* by a CUL-3-independent mechanism. Curr Biol. 2005;15(18):1605–1615.

Mains PE, Kemphues KJ, Sprunger SA, Sulston IA, Wood WB. Mutations affecting the meiotic and mitotic divisions of the early *Caenorhabditis elegans* embryo. Genetics. 1990a;126(3):593–605.

Mains PE, Sulston IA, Wood WB. Dominant maternal-effect mutations causing embryonic lethality in *Caenorhabditis elegans*. Genetics. 1990b;125(2):351–369.

Maruyama R, Velarde NV, Klancer R, Gordon S, Kadandale P, Parry JM, Hang JS, Rubin J, Stewart-Michaelis A, Schweinsberg P, *et al.* EGG-3 regulates cell-surface and cortex rearrangements during egg activation in *Caenorhabditis elegans*. Curr Biol. 2007;17(18):1555–1560.

McCarter J, Bartlett B, Dang T, Schedl T. On the control of oocyte meiotic maturation and ovulation in *Caenorhabditis elegans*. Dev Biol. 1999;205(1):111–128.

McNally FJ, Roll-Mecak A. Microtubule-severing enzymes: from cellular functions to molecular mechanism. J Cell Biol. 2018;217(12):4057–4069.

McNally FJ, Vale RD. Identification of katanin, an ATPase that severs and disassembles stable microtubules. Cell. 1993;75(3):419–429.

McNally K, Audhya A, Oegema K, McNally FJ. Katanin controls mitotic and meiotic spindle length. J Cell Biol. 2006;175(6):881–891.

McNally K, Berg E, Cortes DB, Hernandez V, Mains PE, McNally FJ. Katanin maintains meiotic metaphase chromosome alignment and spindle structure *in vivo* and has multiple effects on microtubules *in vitro*. Mol Biol Cell. 2014;25(7):1037–1049.

Metzger MB, Hristova VA, Weissman AM. HECT and RING finger families of E3 ubiquitin ligases at a glance. J Cell Sci. 2012;125(Pt 3):531–537.

Morreale FE, Walden H. Types of ubiquitin ligases. Cell. 2016;165(1):248.e241.

Motohashi T, Tabara H, Kohara Y. Protocols for large scale *in situ* hybridization on *C. elegans* larvae. In: The C. elegans Research Community WormBook, editor. 2006; p. 1–8

Mullen TJ, Davis-Roca AC, Wignall SM. Spindle assembly and chromosome dynamics during oocyte meiosis. Curr Opin Cell Biol. 2019;60:53–59.

Muller-Reichert T, Greenan G, O'Toole E, Srayko M. The *C. elegans* of spindle assembly. Cell Mol Life Sci. 2010;67(13):2195–2213.

Mutlu B, Chen HM, Moresco JJ, Orelo BD, Yang B, Gaspar JM, Keppler-Ross S, Yates JR, Hall DH, Maine EM, *et al.* Regulated nuclear accumulation of a histone methyltransferase times the onset of heterochromatin formation in *C. elegans* embryos. Sci Adv. 2018;4:eaat6224.

Nithianantham S, Le S, Seto E, Jia W, Leary J, Corbett KD, Moore JK, Al-Bassam J. Tubulin cofactors and Arl2 are cage-like chaperones that regulate the soluble alphabeta-tubulin pool for microtubule dynamics. eLife. 2015;4:e08811.

Pal S, Lant B, Yu B, Tian R, Tong J, Krieger JR, Moran MF, Gingras A-C, Derry WB. CCM-3 promotes *C. elegans* Germline development by regulating vesicle trafficking cytokinesis and polarity. Curr Biol. 2017;27(6):868–876.

Pellettieri J, Reinke V, Kim SK, Seydoux G. Coordinate activation of maternal protein degradation during the egg-to-embryo transition in *C. elegans*. Dev Cell. 2003;5(3):451–462.

Pintard L, Willis JH, Willems A, Johnson J-LF, Srayko M, Kurz T, Glaser S, Mains PE, Tyers M, Bowerman B, *et al.* The BTB protein MEL-26 is a substrate-specific adaptor of the CUL-3 ubiquitin-ligase. Nature. 2003;425(6955):311–316.

Quintin S, Mains PE, Zinke A, Hyman AA. The *mbk-2* kinase is required for inactivation of MEI-1/katanin in the one-cell *Caenorhabditis elegans* embryo. EMBO Rep. 2003;4(12):1175–1181.

Raich WB, Moran AN, Rothman JH, Hardin J. Cytokinesis and midzone microtubule organization in *Caenorhabditis elegans* require the kinesin-like protein ZEN-4. Mol Biol Cell. 1998;9(8):2037–2049.

Romé P, Ohkura H. A novel microtubule nucleation pathway for meiotic spindle assembly in oocytes. J Cell Biol. 2018;217(10):3431–3445.

Sakuma C, Okumura M, Umehara T, Miura M, Chihara T. A STRIPAK component Strip regulates neuronal morphogenesis by affecting microtubule stability. Sci Rep. 2015;5:17769.

Sarkar AA, Zohn IE. Hectd1 regulates intracellular localization and secretion of Hsp90 to control cellular behavior of the cranial mesenchyme. J Cell Biol. 2012;196(6):789–800.

Sato M, Konuma R, Sato K, Tomura K, Sato K. Fertilization-induced K63-linked ubiquitylation mediates clearance of maternal membrane proteins. Development. 2014;141(6):1324–1331.

Schlientz AJ, Bowerman B. *C. elegans* CLASP/CLS-2 negatively regulates membrane ingression throughout the oocyte cortex and is required for polar body extrusion. PLoS Genet. 2020;16(10):e1008751.

Schneider CA, Rasband WS, Eliceiri KW. NIH Image to ImageJ: 25 years of image analysis. Nat Methods. 2012;9(7):671–675. 10.1038/nmeth.2089

Shi Z, Jiao S, Zhou Z. STRIPAK complexes in cell signaling and cancer. Oncogene. 2016;35(35):4549–4557.

Srayko M, Buster DW, Bazirgan OA, McNally FJ, Mains PE. MEI-1/MEI-2 katanin-like microtubule severing activity is required for *Caenorhabditis elegans* meiosis. Genes Dev. 2000;14(9):1072–1084.

Srayko M, O'Toole ET, Hyman AA, Muller-Reichert T. Katanin disrupts the microtubule lattice and increases polymer number in *C. elegans* meiosis. Curr Biol. 2006;16(19):1944–1949.

Stitzel ML, Cheng KC, Seydoux G. Regulation of MBK-2/Dyrk kinase by dynamic cortical anchoring during the oocyte-to-zygote transition. Curr Biol. 2007;17(18):1545–1554.

Thompson O, Edgley M, Strasbourger P, Flibotte S, Ewing B, Adair R, Au V, Chaudhry I, Fernando L, Hutter H, *et al.* The million mutation project: a new approach to genetics in *Caenorhabditis elegans*. Genome Res. 2013;23(10):1749–1762.

Tran H, Bustos D, Yeh R, Rubinfeld B, Lam C, Shriver S, Zilberleyb I, Lee MW, Phu L, Sarkar AA, *et al.* HectD1 E3 ligase modifies adenomatous polyposis coli (APC) with polyubiquitin to promote the APC-axin interaction. J Biol Chem. 2013;288(6):3753–3767.

Wang Y, Argiles-Castillo D, Kane EI, Zhou A, Spratt DE. HECT E3 ubiquitin ligases - emerging insights into their biological roles and disease relevance. J Cell Sci. 2020;133:jcs228072.

Wilson KJ, Qadota H, Mains PE, Benian GM. UNC-89 (obscurin) binds to MEL-26, a BTB-domain protein, and affects the function of MEI-1 (katanin) in striated muscle of *Caenorhabditis elegans*. Mol Biol Cell. 2012;23(14):2623–2634.

Xu L, Wei Y, Reboul J, Vaglio P, Shin T-H, Vidal M, Elledge SJ, Harper JW. BTB proteins are substrate-specific adaptors in an SCF-like modular ubiquitin ligase containing CUL-3. Nature. 2003;425(6955):316–321.

Zhang D, Rogers GC, Buster DW, Sharp DJ. Three microtubule severing enzymes contribute to the "Pacman-flux" machinery that moves chromosomes. J Cell Biol. 2007;177(2):231–242.

Communicating editor: V. Reinke